# Carbon and proton Overhauser DNP from MD simulations and *ab initio* calculations: TEMPOL in acetone

## Supporting Information

Sami Emre Küçük[a], Timur Biktagirov[b], and Deniz Sezer[a*]
[a] *Faculty of Engineering and Natural Sciences, Sabancı University, Orhanlı-Tuzla, 34956 Istanbul, Turkey*
[b] *Institute of Physics, Kazan Federal University, 420008 Kazan, Russian Federation*
(Dated: July 27, 2015)

## I. MULTISCALE MODELING OF THE INTERACTIONS BETWEEN THE ELECTRON AND NUCLEAR SPINS

### A. Two-region treatment of the dipolar interaction

Atomically detailed descriptions like molecular dynamics (MD) simulations, while providing a realistic model of the liquid structure and dynamics in the neighborhood of the polarizing agent, are necessarily limited in spatial extent. Due to the long-range nature of the dipolar interaction this may be a serious shortcoming when calculating the dipolar spectral density function (SDF). In contrast, the analytically tractable model of diffusing hard spherical molecules with centered spins (HSCS model)[1,2] easily extends to infinite distances, but may be a poor model of the liquid structure and dynamics in the vicinity of the polarizing agent. Such details are increasingly important for the Overhauser dynamic nuclear polarization (ODNP) at high magnetic fields, which require substantial modulation of the dipolar interaction at short time scales corresponding to frequencies of hundreds of GHz.

Observing that the precise shapes of the molecules and the precise locations of the spins on these molecules are progressively less important with increasing separation between the electron and nuclear spins, Fries *et al.* have proposed a multiscale approach for calculating the dipolar SDF by integrating MD simulations at short spin-spin distances with the hydrodynamic HSCS model at large distances.[3] The idea is to separate the space around the free radical into near and far regions by an imaginary, spherical boundary of radius $d$ during the analysis of the MD simulations (Fig. S1). The time-correlation function (TCF) of the dipolar interaction is then written as a sum of four parts:[3]

$$C_{\mathrm{dip}}(t) = C_{\mathrm{NN}}(t) + C_{\mathrm{NF}}(t) + C_{\mathrm{FN}}(t) + C_{\mathrm{FF}}(t). \quad \text{(S1)}$$

Here, $C_{\mathrm{NF}}(t)$ accounts for the contribution of molecules that are in the near region (N) at some time and are in the far region (F) time $t$ later. Similarly, $C_{\mathrm{NN}}(t)$ is the contribution of molecules that are in the near region both at the beginning and at the end of a time interval of duration $t$. (Transient visits to F are allowed as long as the molecule is back in N at the end of the time interval.)

The proposal of ref. 3 is to estimate the TCFs with at least one subscript N using an atomistic model, and to calculate $C_{\mathrm{FF}}(t)$ using an analytical expression derived from the HSCS model. In this way, both the molecular detail and the contribution of many distant molecules is taken care of. Because $C_{\mathrm{FN}}(t) = C_{\mathrm{NF}}(t)$,[3] what is to be calculated can be summarized as

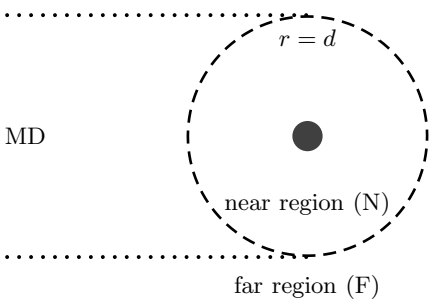


FIG. S1. Partitioning of the space around the polarizing agent (dark circle) into near ($r < d$) and far ($r > d$) regions on the basis of the distance $r$ between the free radical and the solvent molecule.[3]

$$C_{\mathrm{dip}}(t) = C^{\mathrm{MD}}_{\mathrm{NN}}(t) + 2C^{\mathrm{MD}}_{\mathrm{NF}}(t) + C^{\mathrm{HSCS}}_{\mathrm{FF}}(t), \quad \text{(S2)}$$

where the superscripts indicate the model to be employed for the calculation of the respective contribution to the dipolar TCF. Taking the one-sided Fourier transform [defined in eqn (8) of the main text] of both sides of (S2) produces an equivalent decomposition for the dipolar SDF:

$$J(\omega) = J^{\mathrm{MD}}_{\mathrm{NN}}(\omega) + 2J^{\mathrm{MD}}_{\mathrm{NF}}(\omega) + J^{\mathrm{HSCS}}_{\mathrm{FF}}(\omega). \quad \text{(S3)}$$

While the analysis of the MD trajectories results in an estimate of the TCFs, the analytical solution of the HSCS model leads directly to the SDFs. Because the calculation of the relaxation rates $\sigma^S_I$ and $\rho^S_I$ according to Eqs. (5) and (6) in the main text requires $J(\omega)$, the TCFs obtained from the MD trajectories eventually need to be Fourier-transformed numerically and used in (S3).

Attempts to employ the outlined approach in practice, however, face the following problem. According to (S2), the $C_{\mathrm{NF}}(t)$ part of the dipolar TCF should be estimated from MD simulations because the contributing molecular trajectories start in the near region. On the other hand,

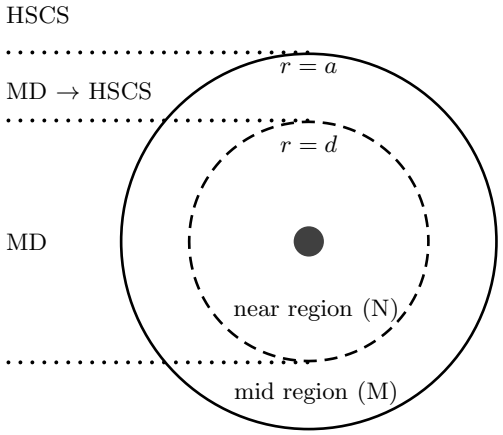


FIG. S2. Partitioning of the space around the polarizing agent (dark circle) into near ($r < d$) and mid ($d < r < a$) regions, where the boundary $r = a$ is absorbing.[4]

the contributing trajectories end in the far region, which extends well beyond the finite spatial dimensions of the MD simulation box all the way to infinity. While the analytical HSCS model is the method of choice when dealing with this far region, it is not expected to be appropriate for handling the near region. Thus, both the atomically detailed and the hydrodynamic descriptions appear to be inappropriate for one of the regions involved in the calculation of $C_{\rm NF}(t)$.

In an effort to address this issue, and thus devise a way of combining the MD simulations with the HSCS model, the finite size of the MD simulation box was explicitly acknowledged in ref. 4. This was done by introducing a spherical outer boundary of radius $a$ that was taken as absorbing, i.e., once a molecule exits the space enclosed by this boundary it is imagined to disappear during the estimation of TCFs from the MD trajectories (Fig. S2). As a result, an intermediate region (M) spanning distances $d < r < a$ from the free radical is defined. In contrast to $C_{\rm NF}(t)$ whose estimation from the MD simulations is problematic due to the infinite spatial extent of region F, $C_{\rm NM}(t)$ can be estimated faithfully from the MD simulations because both regions defined in Fig. S2 are finite in size.

The numerical Fourier transform (FT) of the estimated $C^{\rm MD}_{\rm NM}(t)$ produces an MD estimate of $J_{\rm NM}(\omega)$, the near-intermediate part of the dipolar SDF. [This is represented by the first step in (S4) below.] Thus, we have managed to calculate $J_{\rm NM}(\omega)$ from the MD simulations. However, what is actually needed in (S3) is $J_{\rm NF}(\omega)$ for an infinitely large region F. A prescription for calculating $J_{\rm NF}(\omega)$ from $C^{\rm MD}_{\rm NM}(t)$ was proposed in ref. 4. It may be depicted as follows:

$$C^{\rm MD}_{\rm NM}(t) \overset{\rm FT}{\to} J^{\rm MD}_{\rm NM}(\omega) \overset{\rm fit}{\to} J^{\rm HSCSa}_{\rm NM}(\omega) \overset{\rm unfold}{\to} J^{\rm HSCS}_{\rm NF}(\omega). \quad \text{(S4)}$$

The first step in (S4) was described above. The remaining two steps are performed in order to make the transition from $J_{\rm NM}(\omega)$ to $J_{\rm NF}(\omega)$, i.e., to "unfold" the intermediate region to infinity. First, the MD estimate $J^{\rm MD}_{\rm NM}(\omega)$ is fit by an analytical expression for the near-mid SDF obtained from a finite version of the HSCS model with an absorbing boundary at $r = a$ (denoted by HSCSa). This model with absorbing outer boundary has been examined previously,[5] but was devised and solved independently in ref. 4 with the purpose of bridging the gap between MD simulations and the HSCS model. The analytical expression of $J^{\rm HSCSa}_{\rm NM}(\omega)$ contains the constants $d$ and $a$ that were used in the analysis of the MD simulations, as well as the parameters $b$ and $D$ that are part of the original HSCS model.

In the last step of (S4), the "unfolding" of $J^{\rm HSCSa}_{\rm NM}(\omega)$ to infinite space is achieved by calculating the near-far dipolar SDF using the analytical expression of $J_{\rm NF}(\omega)$, derived from the original HSCS model,[3] with the best-fitting parameters $b$ and $D$ (and the constant $d$). This step is essentially the limit

$$\lim_{a\to\infty} J^{\rm HSCSa}_{\rm NM}(\omega) \to J^{\rm HSCS}_{\rm NF}(\omega). \quad \text{(S5)}$$

As a result, $J_{\rm NF}(\omega)$ obtained in this way is an HSCS-expanded version of the finite-size MD estimate, which may be denoted as $J^{\rm MD\to HSCS}_{\rm NF}(\omega)$.

On first sight, the estimation of the near-near TCF from MD trajectories should not suffer from the difficulty outlined for $C_{\rm NF}(t)$. After all, the trajectory fragments that contribute to $C_{\rm NN}(t)$ start and end in the near region which, unlike F, is finite in extent to begin with (Fig. S1). However, as mentioned before, when calculating $C_{\rm NN}(t)$ only the endpoints of the trajectory fragments of duration $t$ are required to be in region N. As long as this condition is satisfied, in between the trajectories may visit region F one or more times. Faithfully sampling these transient visits to an infinitely large spatial region poses a similar problem to finite-size MD simulations, although the associated error in the estimate of $C_{\rm NN}(t)$ is expected to be much less than that of $C_{\rm NF}(t)$. Next, we describe how the prescription followed to extend the MD estimate of $J_{\rm NM}(\omega)$ to infinite size was adapted to the "unfolding" of the near-near SDF.

Because the unfolding from finite to infinite size is achieved through the HSCS model, in the analysis of the NN part of the dipolar TCF we attempt to separate the HSCS-like dynamics from the actual dynamics. This is done by calculating two different MD estimates for $C_{\rm NN}(t)$, again treating the boundary at $r = a$ as absorbing. In one of them, to be denoted by $C^{\rm MD}_{\rm NN}(t)$, the actual atomic positions are used as proxies of the spin locations. In the other, to be denoted by $C^{\rm COM}_{\rm NN}(t)$, the electron and nuclear spins are imagined to be located at the centers of mass (COM) of the free radical and solvent molecules, respectively. This last choice is expected to reflect the centered-spins (CS) assumption of the HSCS model. The difference between these two estimates reflects the deviation of the actual near-near TCF from its COM approximation:

$$C^{\rm MD}_{\rm NN}(t) = C^{\rm dev}_{\rm NN}(t) + C^{\rm COM}_{\rm NN}(t). \quad \text{(S6)}$$

The unfolding is performed only for the COM part following the same steps as for the NF contribution [*cf.* (S4)]:

$$C_{\mathrm{NN}}^{\mathrm{COM}}(t) \overset{\mathrm{FT}}{\to} J_{\mathrm{NN}}^{\mathrm{COM}}(\omega) \overset{\mathrm{fit}}{\to} J_{\mathrm{NN}}^{\mathrm{HSCSa}}(\omega) \overset{\mathrm{unfold}}{\to} J_{\mathrm{NN}}^{\mathrm{HSCS}}(\omega). \tag{S7}$$

Again, because the resulting $J_{\mathrm{NN}}^{\mathrm{HSCS}}(\omega)$ is an HSCS-expanded version of the finite-size COM estimate, it may be denoted as $J_{\mathrm{NN}}^{\mathrm{COM}\to\mathrm{HSCS}}(\omega)$.

At this point let us comment on the apparent use of different prescriptions when unfolding the NM and NN contributions to the dipolar SDF [*cf.* (S4) and (S7)]. While for NN we distinguished between the COM and the actual TCFs, this was not done for NM. The reason lies in observations from our previous work that, for a sufficiently large $d$, $C_{\mathrm{NM}}^{\mathrm{MD}}(t) \approx C_{\mathrm{NM}}^{\mathrm{COM}}(t)$.[6,7] (This is also seen in Figs. S5b and S6b where the actual and COM estimates of the SDFs coincide.) In other words, for $d$ larger than several times the molecular radii, the NM contribution to the dipolar TCF calculated with the spins assumed to be at the molecular COMs is practically the same as the one calculated with the spins at their actual positions.[8] Thus, for NM the deviation from the COM estimate is equal to zero. Therefore, instead of $C_{\mathrm{NM}}^{\mathrm{MD}}(t)$ in (S4), which is calculated using the actual positions of the spins, we might as well write

$$C_{\mathrm{NM}}^{\mathrm{COM}}(t) \overset{\mathrm{FT}}{\to} J_{\mathrm{NM}}^{\mathrm{COM}}(\omega) \overset{\mathrm{fit}}{\to} J_{\mathrm{NM}}^{\mathrm{HSCSa}}(\omega) \overset{\mathrm{unfold}}{\to} J_{\mathrm{NF}}^{\mathrm{HSCS}}(\omega) \tag{S8}$$

without affecting the final estimate of $J_{\mathrm{NF}}^{\mathrm{HSCS}}(\omega)$. Now (S8) and (S7) look identical.

As mentioned above, the "unfolding" of $J_{\mathrm{NN}}(\omega)$ is necessary because some trajectory fragments of length $t$ that start and end in region N do visit region F in between. Such visits, however, are not entirely missed by the finite-size MD simulations. In fact, all excursions out of region N that remain within $r < a$, i.e., are limited to region M in Fig. S2, are properly accounted for in the MD simulations. It is only rare excursions from $r < d$ to $r > a$ and back to $r < d$ within time $t$ that are made up for by the unfolding procedure. The unfolding step relies on the HSCS model to predict the contribution of excursions from N to F and back to N on the basis of the contribution of the excursions from N to M and back that are actually observed in the MD trajectories. Thus, in a sense, the HSCS model extrapolates from the (observed) N→M→N contribution to the (partly observed) N→F→N contribution.

We, therefore, realize two things. First, for a sufficiently large intermediate region (M) the MD estimate of $J_{\mathrm{NN}}(\omega)$ would be practically unchanged by the unfolding. Second, because the correction is due to trajectory fragments that go outside region N, for $d$ that is several times larger than the molecular radii, the magnitude of the correction should not be very sensitive to the actual location of the spins. Thus, it should be possible to calculate the finite-size correction from $C_{\mathrm{NN}}^{\mathrm{COM}}(t)$, which meets the CS assumption of the HSCS model. In light of these two observations, we calculate the finite-size correction to NN by unfolding only $C_{\mathrm{NN}}^{\mathrm{COM}}(t)$ in (S6) and including the contribution of $C_{\mathrm{NN}}^{\mathrm{dev}}(t)$ as such after calculating its Fourier transform

$$C_{\mathrm{NN}}^{\mathrm{dev}}(t) \overset{\mathrm{FT}}{\to} J_{\mathrm{NN}}^{\mathrm{dev}}(\omega). \tag{S9}$$

At the end, the dipolar SDF is obtained by adding all the separate pieces together:

$$\begin{aligned} J(\omega) = {} & J_{\mathrm{NN}}^{\mathrm{dev}}(\omega) + J_{\mathrm{NN}}^{\mathrm{COM}\to\mathrm{HSCS}}(\omega) \\ & + 2J_{\mathrm{NF}}^{\mathrm{MD}\to\mathrm{HSCS}}(\omega) + J_{\mathrm{FF}}^{\mathrm{HSCS}}(\omega). \end{aligned} \tag{S10}$$

In practice, we write the first two terms on the right-hand side of (S10) as

$$J_{\mathrm{NN}}^{\mathrm{dev}}(\omega) + J_{\mathrm{NN}}^{\mathrm{COM}\to\mathrm{HSCS}}(\omega) = J_{\mathrm{NN}}^{\mathrm{MD}}(\omega) + \Delta_{\mathrm{NN}}^{\mathrm{fs}}(\omega), \tag{S11}$$

where the finite-size correction to $J_{\mathrm{NN}}^{\mathrm{MD}}(\omega)$ was defined as

$$\Delta_{\mathrm{NN}}^{\mathrm{fs}}(\omega) \equiv J_{\mathrm{NN}}^{\mathrm{COM}\to\mathrm{HSCS}}(\omega) - J_{\mathrm{NN}}^{\mathrm{COM}}(\omega). \tag{S12}$$

With the help of the fit in (S7) this correction can be calculated analytically as

$$\Delta_{\mathrm{NN}}^{\mathrm{fs}}(\omega) = J_{\mathrm{NN}}^{\mathrm{HSCS}}(\omega) - J_{\mathrm{NN}}^{\mathrm{HSCSa}}(\omega). \tag{S13}$$

To obtain $J_{\mathrm{NN}}^{\mathrm{MD}}(\omega)$, we perform a multiexponential fit to the NN part of the dipolar TCF calculated from the MD trajectories using the actual locations of the spins:

$$C_{\mathrm{NN}}^{\mathrm{MD}}(t) = \sum_i a_i e^{-t/\tau_i}. \tag{S14}$$

Using the fitting parameters $a_i$ and $\tau_i$ the desired SDF is calculated analytically [see Eq. (8) in the main text]:

$$J_{\mathrm{NN}}^{\mathrm{MD}}(\omega) = \frac{2\pi}{5}(\delta_{IS})^2 \sum_i \frac{a_i\tau_i}{1+(\omega\tau_i)^2}. \tag{S15}$$

### B. Additional quantum region for the scalar interaction

Unlike the dipolar interaction, the scalar interaction is short-ranged. Therefore, for the scalar interaction, any reasonably-sized MD simulation box should automatically be "sufficiently large" such that applying the two-region unfolding procedure described above becomes unnecessary. Thus, it should be possible to base the estimate of $C_{\mathrm{iso}}(t)$ on the scalar TCF calculated from the MD trajectories as such without any finite-size correction.

The Fermi contact depends on the electron spin density at the positions of the nuclei of interest. While the nuclear positions can be obtained from the MD snapshots, the determination of the spatial distribution of the electron spin density requires genuinely quantum mechanical calculations. For the treatment of the scalar interaction, therefore, we introduced a quantum region in which the free radical and a few solvent molecules around

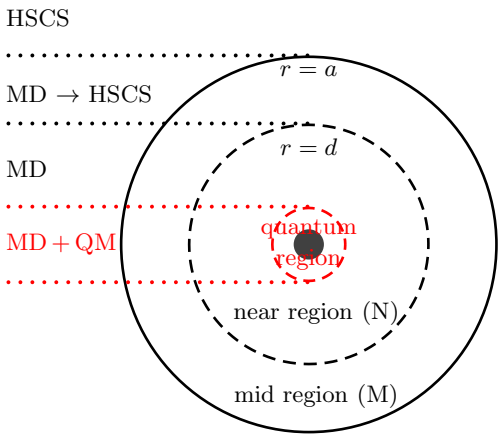


FIG. S3. A schematic depiction of the quantum region (red) containing only a few solvent molecules closest to the oxygen atom of the nitroxide free radical. The scalar interaction is computed with *ab initio* calculations of the molecules in the quantum region as extracted from the MD snapshots. Thus, scalar SDF is obtained by combining the MD simulations with quantum mechanical calculations (MD + QM). The other two regions are necessary for the calculation of the dipolar SDF.

it are modeled in greater (quantal) detail than available from the (classical) MD simulations (Fig. S3). Differently from the near and mid regions introduced previously for the analysis of the dipolar interaction, the quantum region was not defined by a fixed distance from the center of mass of the free radical. Instead, the six solvent molecules whose centers of mass were closest to the nitroxide oxygen atom, as well as the free radical itself, were included in the quantum region. (The choice of six molecules was based on the analysis given in Fig. 2 of the main text.) As a result, in every MD snapshot the spatial extent of the quantum region is slightly different because of the motions of the liquid molecules.[9]

With the quantum region defined as explained, the scalar interaction of a given nucleus with the electron spin is either taken from the *ab initio* calculation if the nucleus is in the quantum region, or is automatically assigned as zero if the nucleus is outside the quantum region. That the scalar interaction does drop to zero even for molecules in the quantum region can be seen from the $A_{\rm iso}$ values of distant nuclei included in the *ab initio* calculation (Fig. 3 in the main text). As a result, $A_{\rm iso}$ values were obtained as a function of time for every proton and carbon nucleus in the MD simulation box. A 30 ps fragment for the $C_{H_3}$ nucleus that was observed to experience maximal positive Fermi contact is shown in Fig. S4.

Scalar TCFs for the proton and carbon nuclei were obtained according to Eq. (9) in the main text. These were then fit to a sum of exponential decays

$$C_{\rm iso}(t) = \sum_i a_i e^{-t/\tau_i}, \tag{S16}$$

which were analytically Fourier-transformed according to

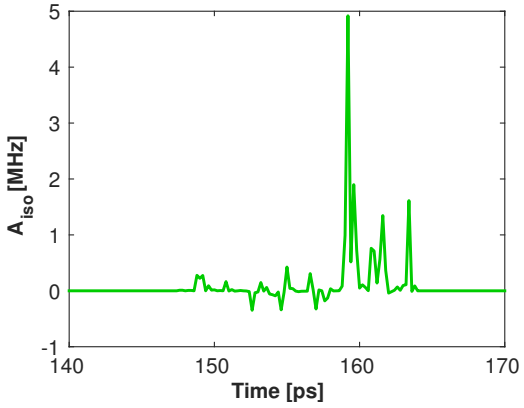


FIG. S4. Fermi contact values of the $C_{H_3}$ nucleus as a function of time. The selected time window includes the point with observed maximum positive $A_{\rm iso}$ value (indicated with asterisk in Fig. 4a of the main text).

Eq. (10) in the main text to obtain the scalar SDF:

$$K(\omega) = \sum_i \frac{a_i \tau_i}{1 + (\omega\tau_i)^2}. \tag{S17}$$

## II. ANALYSIS

### A. Dipolar interaction

In the following we used $d = 2.5$ nm and $a = 3.4$ nm, which were employed in our previous analysis of TEMPOL in acetone.[7] Using the above strategy, dipolar SDFs were calculated for the $C_{H_3}$ and $C_O$ atoms of acetone. The analysis was also repeated for the protons of acetone, which had been analyzed before.[7]

#### 1. *Carbon-electron dipolar interaction*

The NN and NM carbon-electron SDFs calculated from the MD trajectories and the best fits to the COM SDFs with the finite-space HSCS model (HSCSa) are shown in Fig. S5. Note that, with our choice of $d$ and $a$, the actual spin positions on the molecules become immaterial for the MD estimate of $J_{\rm NM}(\omega)$. The "distance of closest approach," $b$, and the coefficient of relative translational diffusion, $D$, that produce the best fits with the HSCSa model are given in the NN and NM columns of Table S1. These parameters are identical to those reported in Table 4 of ref. 7 (for 1 TEMPOL) since they correspond to the same center-of-mass positions. The values in the FF column of Table S1, which are also identical to the ones reported in Table 4 of ref. 7, are not determined from fits to the MD SDFs. Instead, $D$ is obtained as the sum of the TEMPOL and acetone diffusion coefficients as deduced from the MD simulations. The parameter $b$, intended to represent the distance of closest approach of

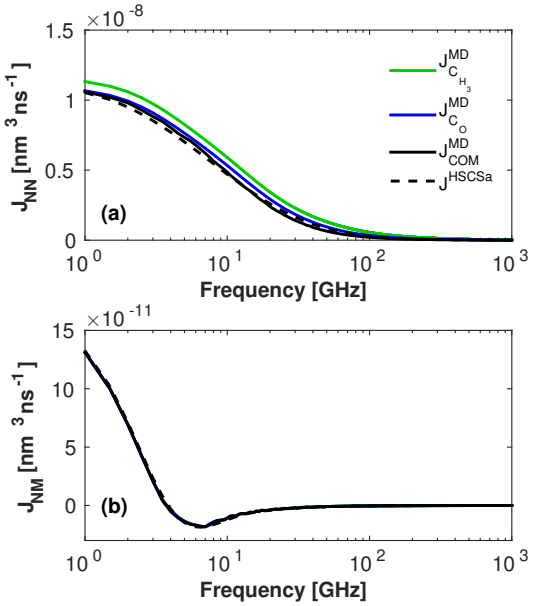


FIG. S5. (a) NN and (b) NM dipolar SDFs between the electron spin and the indicated carbon nuclei of acetone. SDFs of $C_{H_3}$ (green) and $C_O$ (blue) are calculated from the actual positions of the nuclear spins. COM SDFs (black) are calculated pretending that the electron and nuclear spins are at the centers of mass of the TEMPOL and acetone molecules. Best fits to the latter with the HSCSa model are shown with dashed lines.

TABLE S1. The parameters $b$ and $D$ obtained by fitting the COM dipolar SDFs in Fig. S5 with the analytical expressions from the finite-size (absorbing) HSCS model.

| | NN | NM | FF |
|---|---|---|---|
| $b$/nm | 0.45 | 0.40 | 0.51 |
| $D$/nm$^2$ns$^{-1}$ | 5.22 | 6.16 | 8.11 |

the molecules, is taken as the value of $r$ at which the radial distribution function $g(r)$ equals 0.5. (For a plot of the RDF see ref. 7.)

The multi-exponential fit parameters for the NN part of the dipolar TCFs of the three nuclei [see (S14)] are given in Table S2. The fits were performed with the commercial software package MATLAB.[10] When the numbers in the proton columns are compared with the previously reported values for acetone (Table S7 of ref. 7) small numerical differences are observed.[11] The reason is that the fits in our previous work were performed with the free visualization software Grace.[12] The numerical differences in the fitting parameters, however, have a negligible effect on the final results, as revealed by the comparison of the proton ODNP coupling factors reported in Table 2 of the main text and in Table 5 of ref. 7 (values for acetone with 1 TEMPOL).

TABLE S2. Multi-exponential fit parameters for the near-near part of the dipolar interaction between the electron and nuclear spins of $C_{H_3}$, $C_O$ and H .

| $C_{H_3}$ | | $C_O$ | | H | |
|---|---|---|---|---|---|
| $a_i$/nm$^{-3}$ | $\tau_i$/ps | $a_i$/nm$^{-3}$ | $\tau_i$/ps | $a_i$/nm$^{-3}$ | $\tau_i$/ps |
| 1.109 | 0.530 | 0.472 | 0.592 | 2.807 | 0.242 |
| 1.869 | 2.770 | 1.213 | 3.612 | 2.766 | 1.696 |
| 2.296 | 10.89 | 2.126 | 11.45 | 2.609 | 9.231 |
| 0.456 | 41.02 | 0.415 | 42.56 | 0.590 | 36.62 |

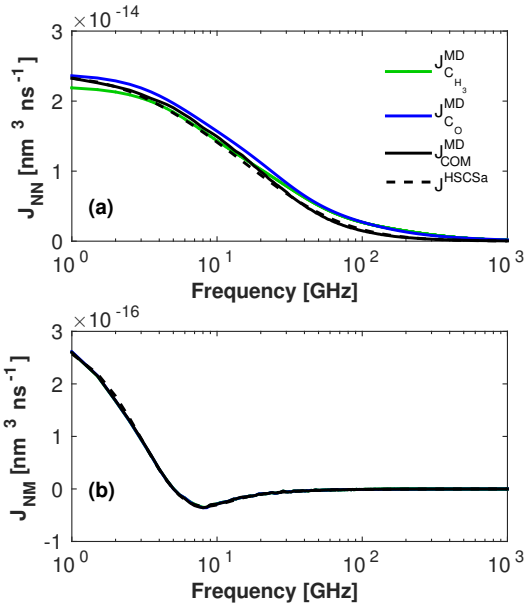


FIG. S6. (a) NN and (b) NM dipolar SDFs between a proton spin and the indicated carbon nuclei of acetone. SDFs of $C_{H_3}$ (green) and $C_O$ (blue) are calculated from the actual positions of the nuclear spins. COM SDFs (black) are calculated pretending that the proton and carbon spins are at the centers of mass of their acetone molecules. Best fits to the latter with the HSCSa model are shown with dashed lines.

### 2. *Carbon-proton dipolar interaction*

The carbon-proton dipolar SDF is necessary to quantify the three-spin effect on the $^{13}$C polarization. In this case, the protocol to calculate the electron-nuclear dipolar SDF was applied in the same manner, except that one randomly chosen acetone molecule was placed at the center of the coordinate system defining the regions in Fig. S2, and the distance vectors from a proton on this acetone to carbon atoms on the remaining acetone molecules were considered. The resulting NN and NM dipolar SDFs are given in Fig. S6. Note that the raw correlation functions are now multiplied by the square of $(\mu_0/4\pi)\hbar\gamma_C\gamma_H$, which leads to orders of magnitude smaller SDFs compared to those in Fig. S5.

The $b$ and $D$ parameters obtained from the fit to the COM dipolar SDFs with the HSCSa model are given in the NN and NM columns of Table S3. These values are

TABLE S3. Parameters $b$ and $D$ from the fit of the carbon-proton COM dipolar SDFs with the HSCSa model as shown in Fig. S6.

| | NN | NM | FF |
|---|---|---|---|
| $b$/nm | 0.38 | 0.40 | 0.42 |
| $D$/nm$^2$ns$^{-1}$ | 7.1 | 7.9 | 10.4 |

TABLE S4. Multi-exponential fit parameters for the NN part of the dipolar TCFs between proton and carbon nuclei.

| $C_{H_3}$ | | $C_O$ | |
|---|---|---|---|
| $a_i$/nm$^{-3}$ | $\tau_i$/ps | $a_i$/nm$^{-3}$ | $\tau_i$/ps |
| 25.337 | 0.001 | 48.385 | 0.221 |
| 82.892 | 0.618 | 55.205 | 1.178 |
| 57.934 | 4.609 | 56.822 | 5.948 |
| 13.307 | 22.19 | 9.196 | 27.14 |

the "distance of closest approach" and the coefficients of relative translational diffusion of two acetone molecules. They differ from the values in Table S1, which are for TEMPOL and acetone. The FF value of $D$ is equal to twice the diffusion coefficient of acetone. The FF value of $b$ is read from the acetone-acetone radical distribution function (see Fig. 2 of ref. 7).

The NN part of the carbon-proton dipolar TCFs were fit to a sum of 4 exponential functions as shown in (S14). The resulting magnitude and decay timescales are given in Table S4. Note that, the way $C_{\rm dip}(t)$ has been defined in Eq. (7) of the main text, its value at $t = 0$ reflects purely geometrical information. The larger sums $\sum_{i=1}^{4} a_i$ in Table S4 compared to the same sums in Table S2 indicate that the protons of acetone come closer to the carbons of other acetone molecules compared to the unpaired electron of TEMPOL.

### B. Scalar interaction

Scalar TCFs were calculated from all the $A_{\rm iso}$ time series, a fragment of one of which is shown in Fig. S4. Coordinates were taken from two, 1 ns-long segments of the MD simulations, whose snapshots were recorded with time step $\Delta t = 0.2$ ps. This implies a frequency bandwidth of $F = 5000$ GHz. The scalar TCFs were calculated for a total duration of $T = 500$ ps, which corresponds to a frequency resolution of $\Delta f = 1$ GHz.

The calculated scalar TCFs for both segments are shown in Fig. S7. Their averages are given in Fig. 5 of the main text. The 1 ns-long MD segments are observed to lead to almost identical scalar TCFs, demonstrating the statistical convergence of $C_{\rm iso}(t)$ estimated by averaging over the two fragments.

These TCFs and their averages were fit to a sum of 4 decaying exponential functions according to (S16). The fits to the separate segments are plotted with dashed black lines in Fig. S7. The fits to the average TCFs

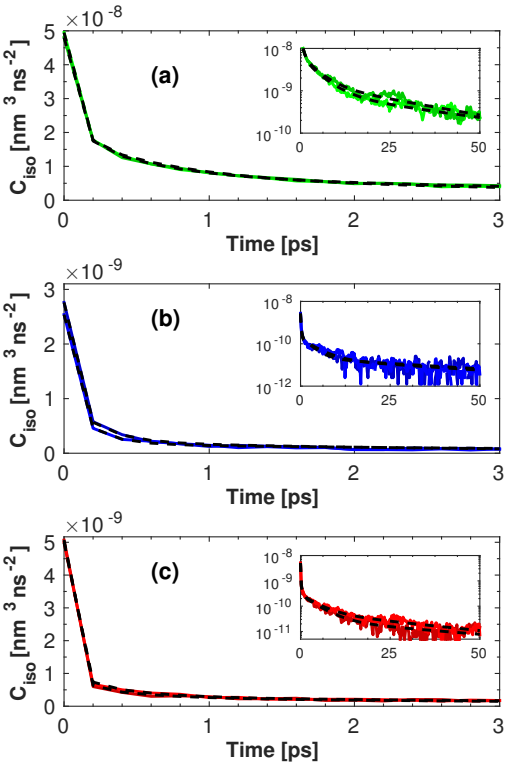


FIG. S7. TCFs for scalar coupling. Fermi contacts are calculated from two different fragments of the MD simulations. They were plotted as straight and their fits are in dashed lines.

are shown with dashed lines in Fig. 5 of the main text. The magnitudes and decay rates of these exponentials are listed in Table S5.

TABLE S5. Multi-exponential fit parameters $a_i$ ($10^{-8}$ nm$^3$ns$^{-2}$) and $\tau_i$ (ps) of the scalar TCFs of the two different fragments and their average.

| | $C_{H_3}$ | | $C_O$ | | H | |
|---|---|---|---|---|---|---|
| | $a_i$ | $\tau_i$ | $a_i$ | $\tau_i$ | $a_i$ | $\tau_i$ |
| first | 3.004 | 0.070 | 0.162 | 0.008 | 0.433 | 0.050 |
| | 1.336 | 0.712 | 0.092 | 0.213 | 0.047 | 0.403 |
| | 0.524 | 4.691 | 0.020 | 2.544 | 0.025 | 4.252 |
| | 0.088 | 37.77 | 0.002 | 43.25 | 0.003 | 38.14 |
| | $C_{H_3}$ | | $C_O$ | | H | |
| | $a_i$ | $\tau_i$ | $a_i$ | $\tau_i$ | $a_i$ | $\tau_i$ |
| second | 2.806 | 0.070 | 0.151 | 0.008 | 0.408 | 0.050 |
| | 1.276 | 0.560 | 0.086 | 0.185 | 0.063 | 0.401 |
| | 0.574 | 3.986 | 0.015 | 3.756 | 0.023 | 4.181 |
| | 0.151 | 28.92 | 0.002 | 40.00 | 0.006 | 30.00 |
| | $C_{H_3}$ | | $C_O$ | | H | |
| | $a_i$ | $\tau_i$ | $a_i$ | $\tau_i$ | $a_i$ | $\tau_i$ |
| average | 2.851 | 0.070 | 0.162 | 0.007 | 0.425 | 0.050 |
| | 1.295 | 0.544 | 0.087 | 0.236 | 0.050 | 0.404 |
| | 0.618 | 4.035 | 0.012 | 3.851 | 0.025 | 4.351 |
| | 0.116 | 33.76 | 0.001 | 60.85 | 0.004 | 33.85 |

ODNP coupling factors were calculated using the scalar SDFs obtained separately from the two 1 ns-long

TABLE S6. DNP coupling factors (%) for $^{13}$C and $^{1}$H at the specified electron/proton Larmour frequencies (GHz/MHz) calculated using the scalar SDFs estimated separately from the first (1) and second (2) trajectory fragments.

| | | 9.7/15 | 34/50 | 94/140 | 260/400 | 460/700 |
|---|---|---|---|---|---|---|
| $C_{H_3}$ | 1 | 21.9 | 7.0 | −0.2 | −1.8 | −1.5 |
| | 2 | 21.4 | 7.3 | 0.3 | −1.7 | −1.5 |
| $C_O$ | 1 | 34.1 | 15.0 | 4.2 | 0.9 | 0.3 |
| | 2 | 34.1 | 15.0 | 4.2 | 0.9 | 0.3 |
| H | 1 | 36.2 | 19.9 | 9.36 | 3.47 | 2.02 |
| | 2 | 36.2 | 19.9 | 9.36 | 3.47 | 2.02 |

trajectory fragments (Table S6). Identical values are obtained for H and $C_O$, for which the dipolar interaction dominates over the scalar interaction. In the case of $C_{H_3}$, which experiences strongest scalar interaction among the three nuclei, the estimates based on the separate trajectory fragments show numerical differences. The magnitude of this difference should give a feeling of the statistical uncertainty associated with the numbers reported in Table 3 of the main text, which were obtained using the estimate of the scalar SDF from the average of the two trajectory fragments.

* dsezer@sabanciuniv.edu


[1] Y. Ayant, E. Belorizky, J. Alizon, and J. Gallice, J. Phys. (Paris) **36**, 991 (1975).

[2] L.-P. Hwang and J. H. Freed, J. Chem. Phys. **63**, 4017 (1975).

[3] P. H. Fries, D. Imbert, and A. Melchior, J. Chem. Phys. **132**, 044502 (2010).

[4] D. Sezer, Phys. Chem. Chem. Phys. **15**, 526 (2013).

[5] B. Halle, J. Chem. Phys. **119**, 12373 (2003).

[6] D. Sezer, Phys. Chem. Chem. Phys. **16**, 1022 (2014).

[7] S. E. Küçük, P. Neugebauer, T. F. Prisner, and D. Sezer, Phys. Chem. Chem. Phys. **17**, 6618 (2015).

[8] The observation $C_{\rm NM}^{\rm MD}(t) \approx C_{\rm NM}^{\rm COM}(t)$ can be viewed as a necessary check of the assumption that $d$ is large enough for the actual location of the spins to be immaterial, justifying the use of the HSCS model during the fitting and unfolding steps.

[9] It is possible to define the quantum region by a fixed distance from the free radical, e.g., $r < q$ for a specified $q$, and allow for a variable number of solvent molecules in successive *ab initio* calculations. For easier bookkeeping we have preferred to deal with fixed number of molecules in the quantum region.

[10] MATLAB, *version 8.4 (R2014b)* (The MathWorks Inc., Natick, Massachusetts, 2014).

[11] The units of $a_i$ in Table S7 of ref. 7 are mistakenly written as nm$^3$. The correct units are 1/nm$^3$.

[12] "Grace," `http://plasma-gate.weizmann.ac.il/Grace/`, [Online; accessed 9-July-2015].